Archives of Medical Research 55 (2024) 102937

ORIGINAL ARTICLE

CETP-derived Peptide Seq-1, the Key Component of HB-ATV-8 Vaccine Prevents Stress Responses, and Promotes Downregulation of Pro-Fibrotic Genes in Hepatocytes and Stellate Cells

Sandra Calixto-Tlacomulco,[a] Ismael Luna-Reyes,[a] Blanca Delgado-Coello,[a] Roxana Gutiérrez-Vidal,[c,d] Juan Pablo Reyes-Grajeda,[b] and Jaime Mas-Oliva[a,*]

[a] *Cellular Physiology Institute, Universidad Nacional Autónoma de México, Mexico City, Mexico*
[b] *Protein Structure Lab, Instituto Nacional de Medicina Genómica, Mexico City, Mexico*
[c] *Researchers Program for Mexico CONAHCYT, Mexico City, Mexico*
[d] *Laboratory of Metabolic Diseases, Cinvestav Unidad Monterey, Apodaca, Nuevo León, Mexico*

Received for publication September 1, 2023; accepted December 14, 2023 (ARCMED-D-23-00730).

Background. The nasal vaccine HB-ATV-8 has emerged as a promising approach for NAFLD (non-alcoholic fatty liver disease) and atherosclerosis prevention. HB-ATV-8 contains peptide seq-1 derived from the carboxy-end of the Cholesteryl Ester Transfer Protein (CETP), shown to reduce liver fibrosis, inflammation, and atherosclerotic plaque formation in animal models. Beyond the fact that this vaccine induces B-cell lymphocytes to code for antibodies against the seq-1 sequence, inhibiting CETP's cholesterol transfer activity, we have hypothesized that beyond the modulation of CETP activity carried out by neutralizing antibodies, the observed molecular effects may also correspond to the direct action of peptide seq-1 on diverse cellular systems and molecular features involved in the development of liver fibrosis.

Methods. The HepG2 hepatoma-derived cell line was employed to establish an *in vitro* steatosis model. To obtain a conditioned cell medium to be used with hepatic stellate cell (HSC) cultures, HepG2 cells were exposed to fatty acids or fatty acids plus peptide seq-1, and the culture medium was collected. Gene regulation of COL1A1, ACTA2, TGF-β, and the expression of proteins COL1A1, MMP-2, and TIMP-2 were studied.

Aim. To establish an *in vitro* steatosis model employing HepG2 cells that mimics molecular processes observed *in vivo* during the onset of liver fibrosis. To evaluate the effect of peptide Seq-1 on lipid accumulation and pro-fibrotic responses. To study the effect of Seq-1-treated steatotic HepG2 cell supernatants on lipid accumulation, oxidative stress, and pro-fibrotic responses in HSC.

Results and Conclusion. Peptide seq-1-treated HepG2 cells show a downregulation of *COLIA1*, *ACTA2*, and *TGF-β* genes, and a decreased expression of proteins such as COL1A1, MMP-2, and TIMP-2, associated with the remodeling of extracellular matrix components. The same results are observed when HSCs are incubated with peptide Seq-1-treated steatotic HepG2 cell supernatants. The present study consolidates the nasal vaccine HB-ATV-8 as a new prospect in the treatment of NASH directly associated with the development of cardiovascular disease.

Key Words: Vaccine HB-ATV-8, NAFDL, Inflammation, Pro-fibrotic genes, Hepatocytes, Hepatic stellate cells.

Address reprint requests to: Biochemistry and Structural Biology Department, Cellular Physiology Institute, Universidad Nacional Autónoma de México, 04510, Mexico City, Mexico; E-mail: jmas@ifc.unam.mx

https://doi.org/10.1016/j.arcmed.2023.102937

Introduction

Non-alcoholic fatty liver disease (NAFLD), which is directly associated with non-alcoholic steatohepatitis (NASH), has recently been identified as metabolic dysfunction-associated steatotic liver disease (MASLD) or metabolic-associated steatohepatitis (MASH). This condition is characterized histologically and metabolically by the excessive accumulation of fat in the liver (1,2), clinically known as steatosis (3,4). NAFLD is closely linked to metabolic disorders, including obesity, insulin resistance, and dyslipidemia, and is recognized as a risk factor for atherosclerosis (5–9). It is characterized by elevated plasma triglyceride levels, increased low-density lipoprotein (LDL) levels, and decreased high-density lipoprotein (HDL) levels, all of which contribute to the development of atherogenesis (10–12).

The mechanisms by which NAFLD leads to liver fibrosis and contributes to atherosclerosis are complex and poorly understood. One proposed mechanism involves the production of pro-inflammatory cytokines by hepatocytes, which may promote endothelial dysfunction and increase the recruitment of inflammatory cells to the arterial wall (13,14). Inflammation, a key driver of atherosclerosis associated with cytokine production by hepatocytes, may exacerbate this process. The involvement of cytokines in the association between fatty liver disease and atherosclerosis is complex and involves both pro- and anti-inflammatory cytokines (13,15,16). Additionally, due to its association with insulin resistance, NAFLD may promote atherosclerosis through the accumulation of advanced glycation end products (AGEs) in the arterial wall. These AGEs can activate inflammatory pathways that further contribute to plaque formation (17,18), potentially involving interleukins IL-6 and IL-1β, which have been significantly associated with disease progression (19). The production of these pro-inflammatory cytokines appears to be actively suppressed by nitric oxide (NO) through the action of three isoforms of NO synthase (NOS) (20). NOS3 (endothelial NOS) is most abundant in vascular endothelium but has also been found in neurons, epithelial cells, cardiomyocytes, adipocytes, and hepatocytes. NOS2 (inducible NOS) is expressed in multiple cell types in response to inflammatory stimuli (21). In addition, vascular cell adhesion molecules, such as VCAM, ICAM, and E-selectin, which are expressed by endothelial cells and upregulated in response to inflammatory signals, are known to regulate leukocyte adhesion to the endothelium and mediate inflammation in NAFLD (22).

While hepatocytes are the primary functional cells of the liver responsible for many of its metabolic and detoxification functions, hepatic stellate cells (HSCs) are mesenchymal cells that reside in a quiescent state in the normal liver and contain abundant lipid droplets of vitamin A and retinoids (23–25). Upon liver injury, HSCs are activated and lose their vitamin A content, changing their phenotype to α-smooth muscle actin (α-SMA)-positive myofibroblasts. These activated HSCs acquire proliferative, contractile, migratory, and fibrogenic properties. These processes are involved in the production of extracellular matrix proteins, matrix-degrading metalloproteinases, and increased amounts of pro-inflammatory and pro-fibrogenic cytokines, ultimately leading to the development of liver fibrosis. Through the space of Disse, hepatocytes communicate with HSCs, allowing these cells to respond to hepatocyte signals (25,26).

One important signal that hepatocytes provide to HSCs is through transforming growth factor-beta (TGF-β), which promotes HSC activation and proliferation. While HSC activation is a normal response to liver injury, prolonged or excessive activation can lead to liver fibrosis, which is characterized by the excessive accumulation of extracellular matrix (ECM) proteins in the liver. This process can ultimately lead to cirrhosis and liver failure (27–29).

Due to the lack of current treatments for NAFLD and limited treatments for atherosclerosis, there is a need for new therapeutic approaches. Recent studies from our laboratory have shown that administration of the nasal vaccine HB-ATV-8, which contains the peptide Seq-1 (CHLLVDFLQSLS), a small fragment derived from the C-terminal region of the cholesteryl-ester transfer protein (CETP), may be a promising new approach for the prevention of both NAFLD and atherosclerosis (30–32). Preclinical studies in animal models have shown that immunization with the nasal vaccine HB-ATV-8 reduces liver fibrosis, inflammation, and atherosclerotic plaque formation in the arteries (33–36).

The mechanism by which HB-ATV-8 exerts its beneficial effects is thought to involve the presentation of the antigen to B-cell lymphocytes through somatic hypermutation. This process allows B cells to begin coding for a new antibody against the unique epitope of the C-terminal region of CETP (37). Once antibodies with sufficient specificity to the epitope are encoded, the B cells release antibodies that specifically bind to the native peptide seq-1 and inhibit the cholesterol transfer activity of CETP, as the C-terminal region corresponds to the functional region of the protein (37–41,). Additionally, the activation of regulatory T cells (Tregs) and the suppression of pro-inflammatory cytokines may play a vital role in the prevention of NAFLD and atherosclerosis. Tregs are a subset of immune cells that regulate the immune response, and some evidence suggests that their activation may be linked to the production of a unique antibody by B cells (42–44). By promoting the development of Tregs, HB-ATV-8 may help reduce inflammation and prevent the development of NAFLD and atherosclerosis.

Furthermore, we have demonstrated that peptide seq-1 can directly affect cells such as hepatocytes or endothelial cells by downregulating a series of genes involved

in extracellular matrix (ECM) production. This action appears to prevent the process of liver fibrosis, suggesting that the HB-ATV-8 nasal vaccine may represent a promising new approach for treating these common and serious health problems.

Based on the histological results obtained in our laboratory while studying a model of atherosclerosis in rabbits and pigs, we observed a significant decrease in the fibrotic process in the liver when using nasal vaccine HB-ATV-8 (33,34). Therefore, in this study, we developed and examined an *in vitro* model employing the human cell lines HepG2 (hepatocytes) and HSC (stellate cells) to mimic some of the features present in NASH. We investigated the direct effect of the peptide Seq-1, the active component of the vaccine formula, on the downregulation of genes involved in the development of inflammation and fibrosis.

Methods

Cell Culture and Establishment of an In vitro *Steatosis Model*

The HepG2 hepatoma-derived cell line (ATCC HB-8065 Manassas, VA, USA) was grown in Dulbecco's Modified Eagle Medium (DMEM) (Gibco, Billings, MT, USA) supplemented with 10% fetal bovine serum (Gibco, Billings, MT, USA) and 10,000 U/mL of penicillin, 10 mg of streptomycin, and 25 µg/mL of amphotericin B, at 37°C, at an atmosphere of 5% CO_2.

Human hepatic stellate cells (HSC) were obtained from ScienCell Research Laboratories (Carlsbad, CA, USA) (Cat. 5300). As recommended by the laboratory, only ScienCell reagents were used for cell handling. Briefly, cells were cultured in SteCM basal medium supplemented with 2 % fetal bovine serum (Carlsbad, CA, USA), 1% stellate cell growth supplement (Carlsbad, CA, USA), and 1 % antibiotic solution (Carlsbad, CA, USA), at 37°C, 5% CO_2. All culture plates seeded with HSCs were pre-coated with 2 µg/mL poly-L-lysine (Carlsbad, CA, USA). The medium was changed daily until the cells reached 70% confluence. HSCs were then incubated for 72 h with the fatty acid-treated HepG2 supernatant (0.6 mM fatty acids, with or without 100 µg/mL of peptide seq-1) or with a conditioned medium of control cells. After the treatment, cells were collected for total RNA extraction and further analysis of fibrinogenic gene expression.

To induce lipid overload, once HepG2 cells reached 75% confluence, cells were exposed to a mixture of oleic acid and palmitic acid (Merck, Saint Louis, MO, USA) in a 2:1 ratio, respectively, increasing concentrations of the fatty acid mixture (0.05,0.1,0.2,0.4,0.6,0.8, 1, and 2 mM) for 24 h.

Briefly, 100 mM palmitic and oleic acid stock solutions for fatty acid treatment were prepared by dissolving the fatty acids in DMSO. A 10% (w/v) fatty acid-free BSA solution (Merck, Saint Louis, MO, USA) was then prepared in H_2O MilliQ. A 5 mM fatty acid/ 1% BSA solution was obtained by adding the required amount of oleate and palmitate stock solutions to 10% BSA at 55°C for 30 minutes. The solution was filtered under sterile conditions before use. Cell viability for cell seeding for all cell culture experiments was assessed using the trypan blue dye exclusion test (Gibco, Billings, MT, USA). Experimental doses were determined by performing dose curves and evaluating cell viability, which was always higher than 85% compared to control cells (100% viability). The effectiveness of the steatotic model employed in this study has been extensively and successfully used by other groups (45,46).

To obtain a conditioned cell medium to be used in HSC cultures, HepG2 cells were exposed to fatty acids or fatty acids plus peptide seq-1 for 24 h, and the culture medium was collected, centrifuged at 6000 rpm to remove cell debris, sterilized by filtration (0.45 μm pore size filter), and stored in aliquots at –20°C until use.

Determination of the Intracellular Lipid Content by Fluorescence Microscopy

Intracellular lipid content was determined microscopically using Nile red stain (47). 250,000 cells were seeded in a six-well microplate and exposed to fatty acid treatment for 24 h at the following concentrations: 0.05, 0.1, 0.2, 0.4, 0.6, 0.8, 1, and 2 mM. The cells were then washed, permeabilized, and fixed. Intracellular lipids were stained with Nile red (0.5 µg/mL) and were examined using an LSM 800 confocal microscope with a 40x/1.3 objective (Carl Zeiss, Oberkochen, Germany). Due to its solvatochromic properties, we used two emission and excitation spectra (λex = 495/λem = 519 nm and λex = 594/λem = 618 nm) (45–47). The whole staining procedure was performed at room temperature, with the samples protected from direct light. Qualitative data were confirmed by quantitative analysis in which the amount of lipids inside the cells was assessed by applying a fluorimetric approach using ImageJ software (NIH, Bethesda, MD, USA).

Cytotoxicity of Fatty Acid Overload and the effect of Peptide Seq-1

Cell viability was assessed using the neutral red uptake colorimetric assay (48). A density of 1×10^5 HepG2 cells per well was seeded in a 96-well plate and allowed to adhere for 24 h. The cells were treated with increasing concentrations of fatty acids (0.1,0.2,0.4,0.6,0.8,1,2, and 4 mM) for 24 h and then incubated with the neutral red solution (40 µg/mL). Finally, the absorbance of each well was read at 540 nm in a Synergy HTX microplate reader (BioTek Instruments Inc., Winooski, VT, USA). The absorbance of untreated (control) cells was 100% survival.

Data are expressed as the mean ± S.E. of six independent experiments. Cells were distributed into a control group of cells incubated with supplemented DMEM only and cells to which the lipid solution was added at different concentrations.

Since the fundamental point of this work is to evaluate the effect of the peptide seq-1 on gene regulation in liver cells, once the concentration of fatty acids to induce a pro-fibrotic response was determined, a subsequent analysis was performed to determine the concentration of peptide to be used. A 5 mg/mL stock solution of the peptide seq-1 (GeneScript, Piscataway, NJ, USA) was dissolved in carbonate buffer ($NaHCO_3/Na_2CO_3$ 50 mM pH 9.5). Cells were stimulated with different concentrations of the peptide (0.0001, 0.001, 0.01, 0.1, 1, 10, 100, and 10000 μg/mL) for 24 h. As described above, cell viability curves were performed with neutral red to determine the experimental dose used throughout the study.

Evaluation of Apoptosis by Flow Cytometry

Early and late apoptosis of control cells, those treated with 0.6 mM fatty acids and those treated with fatty acids plus the peptide seq-1 100 μg/mL, was determined by a two-stain assay and assessed by flow cytometry. Cells were labeled with Annexin V and 7-amino actinomycin D (7AAD). To ensure the consistency of flow cytometry data and to compensate for fluorophore cross-linking, a single staining of each dye (Annexin V and 7-AAD) was performed for each preparation. Briefly, cells were harvested by gentle trypsinization, washed, and the pellet was suspended in DMEM. 2×10^3 cells were incubated with 5 μL of Annexin V and 5 μL of 7AAD for 30 min at 37°C. Cells were diluted with an incubation buffer and analyzed with a Cytoflex S cytometer (Beckman Coulter, Inc. Brea, CA, USA) using a 660/20 nm band-pass filter for Annexin detection (FL6 channel) and a 690/50 nm filter for 7AAD detection (FL4 channel). Data were analyzed using FlowJo software (BD Bioscience, Franklin Lakes, NJ, USA). The same flow cytometry protocol was used for all experiments in the study.

Biochemical Analysis

After obtaining lysates with RIPA from cells treated with 0.6 mM fatty acids and those treated with fatty acids plus the peptide seq-1 100 μg/mL, triglyceride (TG) concentration, total cholesterol (TC), glucose, as well as the enzymatic activity of aspartate aminotransferase (AST), and alanine aminotransferase (ALT), were determined using a Dirui cs-T240 UV-visible spectrophotometer (Dirui Industrial, Jilin, China), using dcL-SEKISUI reagents (SEKISUI, Secaucus, NJ, USA). These studies were performed at the Department of Pathology, Faculty of Veterinary Medicine and Zootechnics, Universidad Nacional Autónoma de México.

Measurement of Intracellular ROS levels using H2DCFDA

To determine whether fatty acid-induced ROS production could be reversed by the peptide seq-1 treatment, cells were co-treated with 0.6 mM fatty acid solution and 100 μg/mL of peptide seq-1. ROS accumulation was determined with the fluorescent probe 2′,7′ -dichlorofluorescein diacetate (H2DCFDA) (Invitrogen, Waltham, MA USA). Briefly, pre-treated cells were incubated with 5 mM H2DCFDA for 30 min at 37°C. Fluorescence intensity was measured using a microplate reader (BioTek Instruments Inc., Winooski, VT, USA) at 485 nm excitation and 530 nm emission.

Expression Analysis of pro-fibrotic and Inflammatory Markers Using Real-time Quantitative PCR

After the indicated treatments, the culture medium was removed, and the cells were lysed with Trizol reagent (*Invitrogen*, Waltham, MA USA). Total RNA was dissolved in nuclease-free water and stored at –20°C until further analysis. RNA was quantified spectrophotometrically, and purity was evaluated by measuring the A260/A280 ratio, considering RNA with appropriate purity values between 1.8 and 2.0. Total RNA was reverse transcribed using the iScript cDNA synthesis kit (Bio-Rad, Hercules, CA, USA), according to the following reaction protocol: five min at 25°C, 20 min at 46°C, and one min at 95°C.

Real-time quantitative PCR was performed on a QuantStudio 7 Flex (Thermo Fisher Scientific, Waltham, MA, USA), using GAPDH as a housekeeping gene. Primer sequences are listed in Table 1. PCR amplification was carried out using PowerUp SYBR Green Master Mix 2X (Thermo Fisher Scientific, Waltham, MA, USA). The dissociation curve analysis showed that non-specific products were amplified. Relative quantification was performed using the $2^{-\Delta\Delta CT}$ method, considering the efficiencies of each gene. The results were normalized to GAPDH and reported as the mean expression ± S.E. of at least three different determinations for each gene.

Immunofluorescence Microscopy of COL1A1, MMP-2 and TIMP-2

HepG2 cells were seeded in 6-well plates, each with a glass slide, and stimulated with 0.6 mM lipid solution and lipid solution plus the peptide seq-1 (100 μg/mL) for 24 h. They were fixed in 4% paraformaldehyde, permeabilized, and blocked, followed by incubation with the anti-COL1A1 (SC-293182), anti-MMP-2 (SC-13594), and anti-TIMP-2 (SC-21735) antibodies 1:50 overnight at 4ºC.

Table 1. Primers designed for the identification of genes associated with liver fibrosis

Gene	Sequence
GAPDH	5′-GCG GGG CTC TCC AGA ACA-3′ (F)
	5′-ACT GAC ACG TTG GCA GTC-3′ (R)
COL1A1	5′-CGA CGG GAG CAG CAT TAG-3′ (F)
	5′-GCG CAG GGG CAA AAT TCG-3′(R)
ACTA2	5′-AGC TGG GGC AGT TGG GTC-3′ (F)
	5′- TGG CCC CAG AGC TGG TAA-3′ (R)
TGFß	5′-ACA GGT TCC TGC TGT GTC-3′ (F)
	5′-CCA TCC TGC ATG CCT CCC-3′ (R)
ICAM	5′-GTA GCA GCC GCA GTC ATA AT-3′ (F)
	5′-GGG CCT GTT GTA GTC TGT ATT T-3′ (R)
VCAM	5′-GAT TGG TGA CTC CGT CTC ATT-3′ (F)
	5′-CCT TCC CAT TCA GTG GAC TAT C-3′ (R)
SELECTIN	5′-CTC AGT GTT CCC TTT CCT ACT C-3′ (F)
	5′-GAG TCT TGG TCT CTT CAC CTT T-3′ (R)
NOS2	5′-GTC AGA GTC ACC ATC CTC TTT G-3′ (F)
	5′-GCA GCT CAG CCT GTA CTT ATC-3′ (R)
NOS3	5′-GGT AGA TTC CTC TTG CCT CTC TC-3′ (F)
	5′-GGC ACA GTC CCT TAT GGT AAA-3′ (R)
IL-10	5′-TTT CCC TGA CCT CCC TCT AA-3′ (F)
	5′-CGA GAC ACT GGA AGG TGA ATT A-3′ (R)
IL-1 ß	5′-CAA AGG CGG CCA GGA TAT A-3′ (F)
	5′-CTA GGG ATT GAG TCC ACA TTC AG-3′ (R)
IL-6	5′-GGA GAC TTG CCT GGT GAA A-3′ (F)
	5′-CTG GCT TGT TCC TCA CTA CTC-3′ (R)

F: Forward; R: Reverse.

Subsequently, incubation with goat anti-mouse Alexa 488 Cat. A110011 (Invitrogen, Waltham, MA, USA) 1:5000 was performed. Images were captured using an LSM800 confocal microscope with a 63 X objective.

Statistical Analysis

Unless otherwise specified, all data are expressed as mean ± S.E. of three independent experiments (biological replicates). The Kolmogorov-Smirnov test was used to evaluate the distribution of each group. The significance of differences between more than two groups was calculated using one-way ANOVA, followed by Tukey's post hoc test for normally distributed data, and Kruskal-Wallis and Dunn's test for non-normally distributed data. Comparisons between the two groups were made using one-way student *t*-tests. The Mann-Whitney *U* test was used to compare data with a non-normal distribution. For all analyses, $p < 0.05$ was considered significant. Statistical analysis and figures were performed using Prism 8.0 software (GraphPad Software, San Diego, CA, USA).

Results

Treatment with Oleate and Palmitate Induces Lipid Internalization in HepG2 Cells

To investigate the effect of peptide seq-1 on human steatotic cells, we established an *in vitro* model that mimics the steatosis process in fatty livers, induced by a 2:1 mixture of oleate and palmitate. Fatty acids were added to a 1% BSA solution to obtain a 6:1 molar ratio (fatty acids/BSA), mimicking hyperlipidemic conditions.

Cell exposure to 0.05, 0.1, 0.2, 0.4, 0.6, 0.8, 1, and 2 mM oleate/palmitate 2:1 for 24 h induced a dose-dependent lipid accumulation (Figure 1A and 1B). Confocal microscopy images show increased lipid droplets in response to fatty acid treatment. Internalization is evident after oleate/palmitate 0.2 mM, where the amount of cytoplasmic lipid droplets increased compared to that observed at lower doses (Figure 1A). Qualitative findings were confirmed by a fluorometric approach using ImageJ software (Figure 1B). It was observed that the increase in cell fluorescence is proportional to the concentration of fatty acids. We found a 3-fold increase (± 2.3; $p = 0.0005$) in fluorescence after incubation with 0.6 mM fatty acids compared to control cells. The lipid accumulation was even more pronounced after exposure to 2 mM palmitate for 24 h (5 ± 6.8-fold increase over control, $p < 0.0001$.

Cell Viability During the Establishment of an In vitro *Model of Steatosis*

The effect of lipid treatment on cell viability was evaluated by measuring neutral red absorbance at 540 nm. The results show that HepG2 cells were sensitive to elevated concentrations of fatty acids, with a decrease in cell viability from a concentration of 1.2 mM ($p < 0.0001$) compared to the control (Figure 2A). Therefore, the 0.6 mM

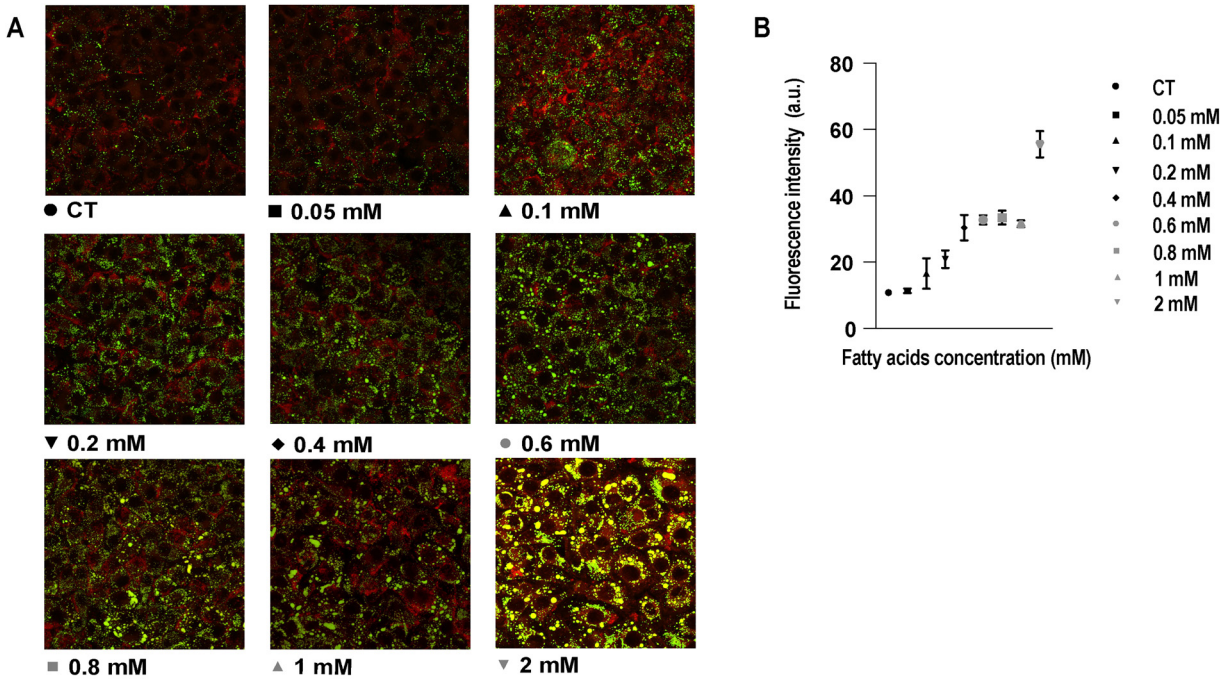

Figure 1. Intracellular lipid accumulation after oleate/palmitate stimulation. A. Human hepatoma HepG2 cells were incubated with increasing concentrations of oleate/palmitate (CT, 0.05 mM, 0.1 mM, 0.2 mM, 0.4 mM, 0.6 mM, 0.8 mM, 1 mM, and 2 mM) for 24 h. Cells without fatty acid treatment served as controls. Cytoplasmic lipid droplets are shown in green: Nile Red staining, images acquired by confocal microscopy. B. Fluorometric assessment of intracellular lipid content. The data represent the mean of the fluorescence intensity values ± the S.E.

fatty acid mixture was selected for subsequent experiments to achieve maximal lipid over-accumulation with minimal cytotoxicity. In this assay a 0.1% Triton X-100 solution was used as a positive control; a cytotoxicity curve was also used to determine the dose.

The effect of peptide seq-1 on the viability of HepG2 cells was also evaluated.A wide range of concentrations (0.0001,0.001,0.01,0.1,1,10,100, and 1000 μg/mL) was tested, and we did not observe a significant decrease in viability at any of the concentrations evaluated (Figure 2B). The effect of peptide seq-1 on cell proliferation was also measured using the neutral red assay. The results showed that the concentration (100 μg/mL) was safe in the subsequent experiments.

To confirm the cell viability results, both HepG2 cells stimulated with 0.6 mM fatty acids and those treated with peptide seq-1100 μg/mL were stained with Annexin V and 7AAD to evaluate early and late apoptosis. According to cell staining, cells were classified as a) live cells, negative for both Annexin-V and 7AAD; b) early apoptotic cells, positive for Annexin-V and negative for 7AAD; and c) late apoptotic cells, positive for both Annexin-V and 7AAD; cells positive for 7AAD only were considered necrotic. The evaluation showed that the percentage of apoptotic cells in the control, steatosis, and the peptide seq-1 treated groups was 2.64, 2.53, and 2.41%, respectively. As shown in Figure 2D, the 0.6 mM concentration of fatty acids did not increase the percentage of cells in early apoptosis (2.53%) or late apoptosis (1.61%), and there was 0.12% in the necrotic population. Similarly, peptide seq-1 did not increase the percentage of cells in early apoptosis (2.41%), late apoptosis (1.57%), or necrosis (0.20%) (Figure 2E).

Peptide seq-1 Regulates the Synthesis of Intracellular Lipids and Attenuates Glucose Accumulation in HepG2 Cells

An assay to measure the intracellular content of cholesterol and triglycerides in HepG2 cells revealed that cells treated with 0.6 mM fatty acids for 24 h (Lipid Tx group) were significantly increased compared to those in the control group ($p = 0.0018$ and $p < 0.0001$, respectively), (Figure 3A), suggesting that fatty acid treatment successfully induces cholesterol and triglyceride synthesis in this cell type. In contrast, it was observed that peptide seq-1 treatment promoted the reduction of intracellular concentrations of cholesterol and triglycerides in fatty acid-treated HepG2 cells ($p = 0.0031$; $p < 0.0001$, respectively) (Figure 3A, and 3B).

To analyze the effect of the peptide seq-1 on glucose metabolism, glucose levels in HepG2 cells were measured. After the addition of fatty acids to the cell culture medium, the intracellular glucose content of the cells increased significantly compared to the control cells ($p = 0.0847$), while the extracellular glucose content decreased 10-fold compared to the control ($p = 0.0011$). The addition of 100

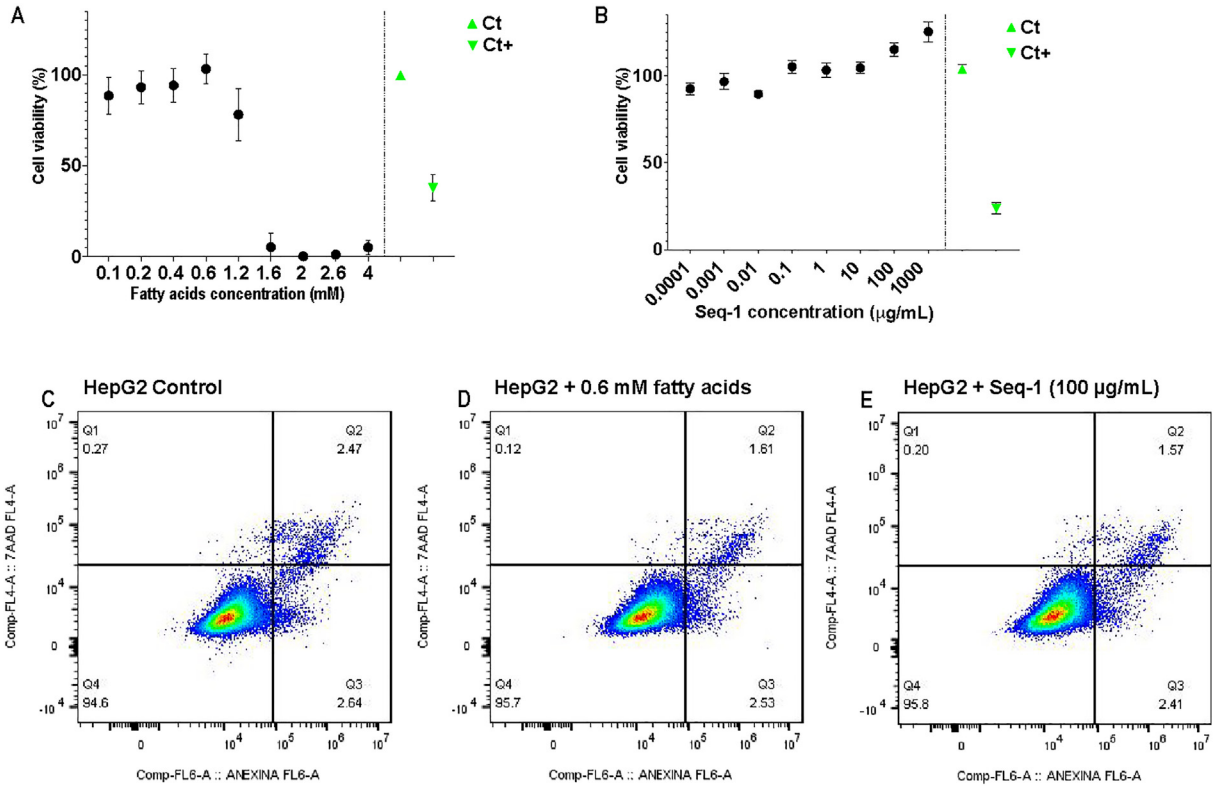

Figure 2. Treated cells viability. A. Cell viability (logarithmic dose-response curves) for HepG2 cells treated for 24 h with increasing concentrations of fatty acids. (oleate/ palmitate 2:1). B. Peptide seq-1 treatment. Data represent the mean ± S.E. Symbols in green represent the controls: Ct (untreated cells); Ct+ (cells + Triton X-100 0.1 %). Flow cytometry detected the apoptosis rate by staining with Annexin-V/7-AAD after treatment for 24 h. Early apoptotic cells stain positive for Annexin V and negative for 7-AAD, late apoptotic cells stain positive for both 7-AAD and Annexin V. Fatty acid overload 0.6 mM, and the peptide seq-1 treatment 100 ug/mL do not alter cell apoptosis C–E.

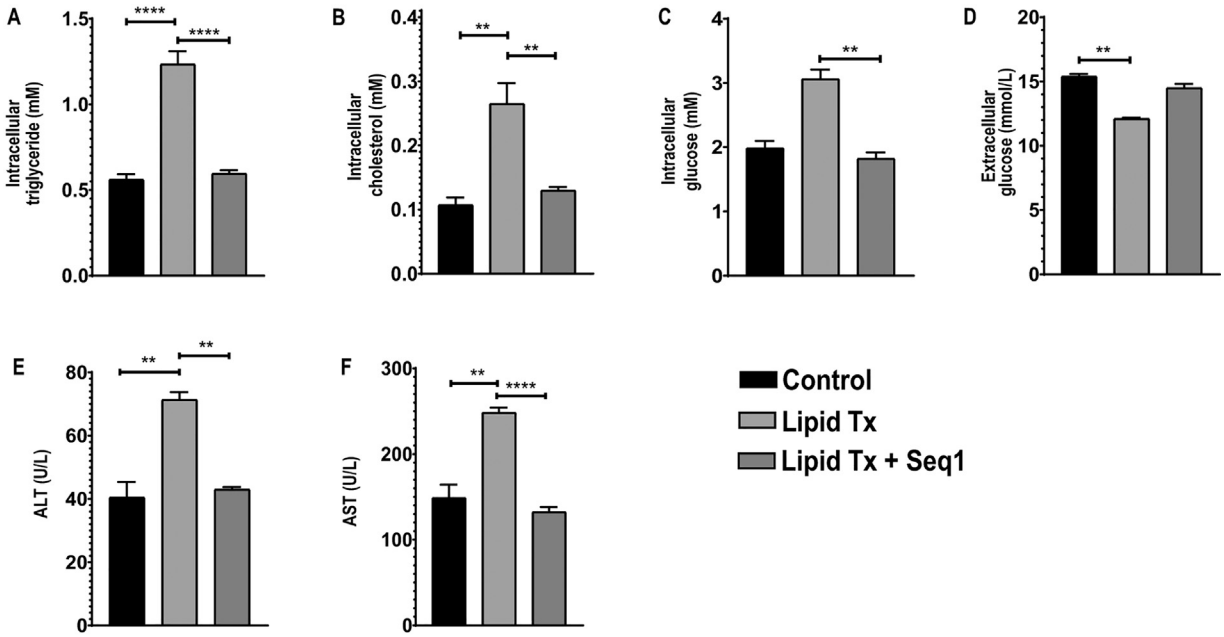

Figure 3. Effect of peptide seq-1 on the intracellular concentration of cholesterol, triglycerides, glucose, as well as extracellular levels of ALT and AST in steatotic HepG2 cells. Control (untreated cells); Lipid Tx (cells incubated with 0.6 mM fatty acids); Lipid Tx+Seq-1 (HepG2 cells + fatty acid treatment 0.6 mM + Seq-1 100 µg/mL). Plotted values represent the mean value ± S.E. $^{**}p$ <0.01; $^{****}p$ <0.0001.

μg/mL of peptide seq-1 to the culture media, allowed the glucose content of the cells to be maintained at normal control levels (Figure 3C). Interestingly, the extracellular glucose level followed the opposite direction, first showing a significant reduction with lipid treatment, a result that is reversed when the cells are further treated with the peptide seq-1 (Figure 3D).

In addition, associated with this phenomenon, there is also a significant increase in AST (99.42 ± 16.42 $p = 0.0019$) and ALT (30.85 ± 5.412 $p = 0.0023$) levels in the extracellular medium after 24 h of fatty acid stimulation compared to controls (Figure 3E, 3F). In contrast, after the addition of peptide seq-1 (100 μg/mL) to the medium, both AST (115.8 ± 8.021, $p < 0.0001$) and ALT (71.33 ± 43.04, $p = 0.0002$) levels were maintained at normal control levels.

Peptide seq-1 Attenuates Oxidative Stress Induced by Lipid Accumulation in HepG2 Cells

To investigate the effect of peptide seq-1 on the process of oxidative stress in steatotic HepG2 cells, we measured intracellular ROS levels. The results show that lipid treatment (0.6 mM) in HepG2 cells induces a significant increase in ROS levels. Interestingly, the addition of peptide seq-1 during treatment reduces the level of oxidative stress (Figure 4).

Cells treated with 0.6 mM lipid showed a significant ($p < 0.0001$) 1.4 ± 14.22-fold increase in ROS generation compared to untreated control HepG2 cells. When 0.6 mM lipid-treated cells were concomitantly exposed to 100 μg/mL of peptide seq-1, the ROS level decreased ($p = 0.0158$) 1.22 ± 0.12-fold compared to those stimulated with lipids only. This result indicates that the presence of peptide seq-1 can reduce the redox state induced by fatty acid treatment.

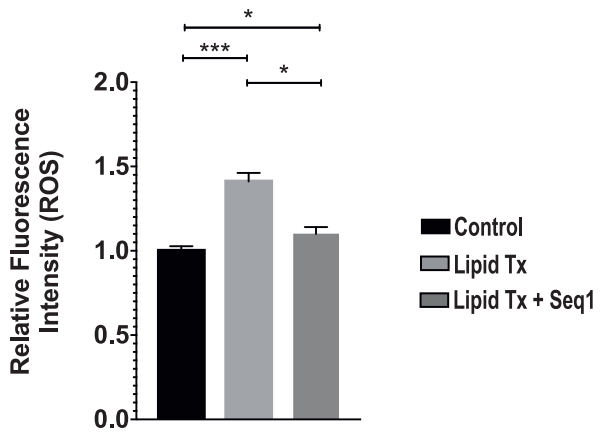

Figure 4. Intracellular ROS formation in HepG2 cells after fatty acids and peptide seq-1 treatment. The relative levels of intracellular ROS of the two treatments are shown. CT (untreated cells); Tx-Lipids (cells incubated with 0.6 mM fatty acids); Tx-Lipids+Seq-1 (HepG2 cells + fatty acid treatment 0.6 mM + Seq-1 at a 100 μg/mL concentration). Relative fluorescence levels were normalized against control (untreated cells). Data are mean ± S.E. representation. $^{*}p < 0.05$; $^{***}p < 0.0001$.

Peptide seq-1 Promotes a Decreased Pro-fibrogenic and Inflammatory Cytokine Gene Expression in HepG2 Cells

Next, we analyzed the effect of peptide seq-1 on gene expression in fatty acid-stimulated HepG2 cells. The mRNA expression of two established markers of HSC activation, type I collagen (COL1A1) and alpha-smooth muscle actin (ACTA2), was determined by quantitative RT-PCR analysis. HepG2 cells stimulated with 0.6 mM fatty acids showed a higher expression of type I collagen (1.57 ± 0.17, $p = 0.340$; Figure 5A) and ACTA2 (1.3 ± 0.563, $p = 0.981$; Figure 5B) expression compared to control HepG2 cells.

Interestingly, COL1A1 and ACTA2 levels decreased significantly in the lipid-stimulated group in the presence

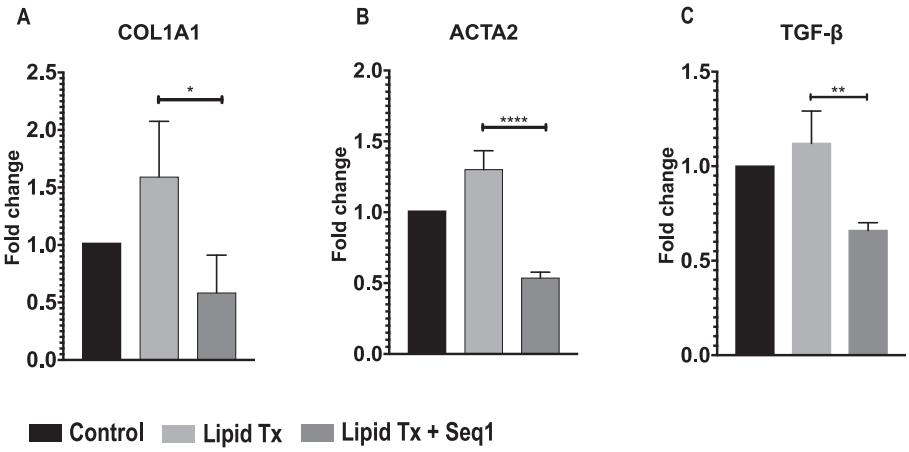

Figure 5. Peptide seq-1 negatively regulates the expression of COL1A1, ACTA2, and TGF-β in steatotic HepG2 cells. 24 h after treatment, mRNA expression of A. COL1A1, B. ACTA2, and C. TGF-β were analyzed by qPCR analysis. Control (untreated cells); Lipid Tx (cells incubated with 0.6 mM fatty acids); Lipid Tx+Seq-1 (HepG2 cells + fatty acid treatment 0.6 mM + Seq-1 100 μg/mL). $^{*}p < 0.05$; $^{**}p < 0.01$; $^{****}p < 0.0001$.

of peptide seq-1, in contrast to the fatty acid-stimulated group (2.73 ± 0.3280, $p = 0.0010$ and 2.42 ± 0.1741 $p = 0.0456$) (Figure 5A, and 5B). These results confirm the effect of peptide seq-1 in the signaling pathways and genes that are directly involved in the fibrotic process.

To further analyze the effect of peptide seq-1 on the inflammatory process induced by fatty acid overload, TGF-β, a cytokine reported as a marker of fibrosis in NAFLD, was evaluated. As shown in Figure 5C, intracellular lipid accumulation was associated with the upregulation of the TGF-β mRNA ($p = 0.9999$). Nevertheless, when cells were treated with peptide seq-1, a negative regulation of TGF-β was observed (1.73 ± 0.36, $p = 0.0008$), suggesting that peptide seq-1 reduces inflammatory responses regulated by this cytokine.

One of the key points of our investigation is to support the results we have obtained with the HB-ATV-8 vaccine, which has been shown to be effective in reducing fatty liver disease along with the prevention of atherogenesis *in vivo*. For this reason, the effect of the peptide seq-1 as the active component of this vaccine has been used in the present research to study not only the balance between a series of inflammatory cytokines but also the oxidative stress process, using our *in vitro* model of steatosis. Figure 6 shows that although under our working conditions, by PCR we did not find any detectable changes in the expression of the cytokines IL-6 and IL-1β after lipid treatment ; in contrast, IL-10 presents a statistically significant increase, a result that is reversed when the cells are further treated with peptide seq-1. Cell adhesion molecules, which are known to promote *in vivo* the fibrotic process and leukocyte migration to the injury site, again showed no significance between groups under our working conditions. However, since there is an interesting tendency for VCAM and selectin to increase in lipid-treated cells, associated with the fact that peptide seq-1 seems to promote the recovery close to control levels, there is a good basis to further investigate these effects by increasing the number of replicas. Although there are no changes in the level of NOS3 after lipid treatment, the nitric oxide synthase NOS2 appears to be significantly decreased in the lipid-treated cell assay, a result that tends to return to control levels when cells are concomitantly treated with lipids in the presence of peptide seq-1 (Figure 6).

Immunocytochemistry: Peptide seq-1 Regulates the Expression of Extracellular Matrix-associated Proteins

We analyzed the effect of peptide seq-1 treatment in steatotic HepG2 cells by evaluating the expression of three fibrosis-related proteins: COL1A1, MMP-2, and TIMP-2. Compared to control HepG2 cells, fatty acid stimulation induced overexpression of COL1A1 (Figure 7A), MMP-2 (Figure 7B), and TIMP-2 (Figure 7C). Consistent with the downregulation of pro-fibrotic genes after peptide seq-1 treatment, we observed a decrease in the expression of all three proteins, expressed as fluorescence intensity in this assay. Compared to the Tx-Lipid group, the Tx-Lipid+Seq-1 group showed a decrease in COL1A1 (Figure 7A); MMP-2 (Figure 7B), and TIMP-2 (Figure 7C).

The Culture Medium of Steatotic HepG2 Cells Induces HSC Activation

Human HSCs were exposed to the culture media of HepG2 cells with different treatments for 72 h. HSCs exposed to the culture media of steatotic HepG2 cells showed an upregulation of pro-fibrotic genes statistically higher than HSCs treated with the culture media of control hepatocytes: COL1A1 (9.54 ± 2.189, $p = 0.0010$), ACTA2 (17 ± 1.068, $p < 0.0001$). This effect was also observed when the pro-inflammatory cytokine TGF-β was measured (5.690 ± 0.106, $p = 0.0009$) (Figures 8A–8C). In contrast, when HSCs were maintained in the culture media of fatty acid-stimulated HepG2 cells but in the presence of 100 μg/mL of peptide seq-1, we observed a restoration, and found that the expression levels of COL1A1, ACTA2, and TGF-β were statistically decreased: COL1A1 (6.240 ± 1.317, $p = 0.0752$; Figure 8A), ACTA2 (8.262 ± 0.588, $p = 0.0003$; Figure 8B) and TGF-β (3.574 ± 0.676, $p = 0.0190$; Figure 8C). These results suggest that HepG2 cells secrete pro-fibrogenic factors involved in HSC activation, where peptide seq-1 shows the ability to promote a decrease in COL1A, ACTA2, and TGF-β expression, therefore, most likely explaining the regulation of the fibrotic process observed in the *in vivo* experiments.

Since it is crucial to demonstrate that the soluble factors released by steatotic hepatocytes are responsible for the pro-fibrogenic effects observed in HSCs after stimulation with the culture media of fatty acid-treated hepatocytes, we measured the concentration of residual fatty acids present in the media using the Nile Red fluorescent dye. Following this procedure, we did not observe any statistically significant differences between the two fatty acid-treated groups compared to controls (data not shown).

Discussion

This study evaluated the hepatoprotective effect of peptide seq-1 by the regulation of key genes involved in the fibrotic process using an *in vitro* model of liver steatosis. The model successfully induced lipid accumulation in HepG2 cells, mimicking the key features of NASH. As an important component of the nasal vaccine HB-ATV-8, peptide Seq-1 has demonstrated its anti-fibrotic and anti-inflammatory effects, and therefore, its usefulness as a therapeutic agent to modulate the complex and dynamic relationship between hepatocytes and HSCs in NAFLD.

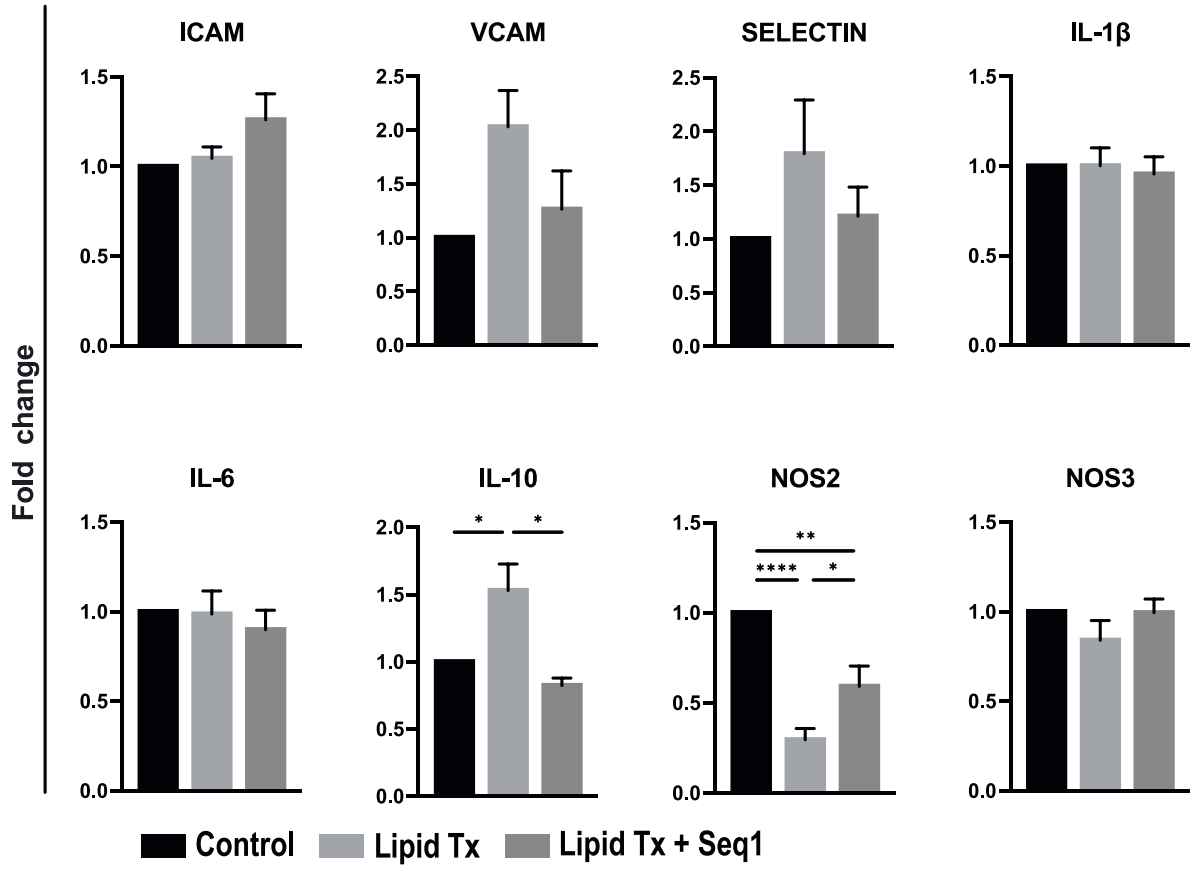

Figure 6. Peptide seq-1-mediated anti-inflammatory response in steatotic HepG2 cells. Analysis of differential expression of ICAM, VCAM, selectin, IL-10, IL-6, IL-1β, NOS2, and NOS3 in comparison to control groups by real-time PCR. Gene expression values were normalized using GAPDH as an endogenous reference gene. Control (untreated cells); Lipid Tx (cells incubated with 0.6 mM fatty acids); Lipid Tx+Seq-1 (HepG2 cells + fatty acid treatment 0.6 mM + Seq-1 100 μg/mL). Statistical analysis was performed with a one-way analysis of variance with an accompanying Tukey's post hoc test for multiple comparisons: $^{*}p$ <0.05, $^{**}p$ <0.01, **** <p 0.0001. Data are expressed as means with SEMs (n = 15 per group).

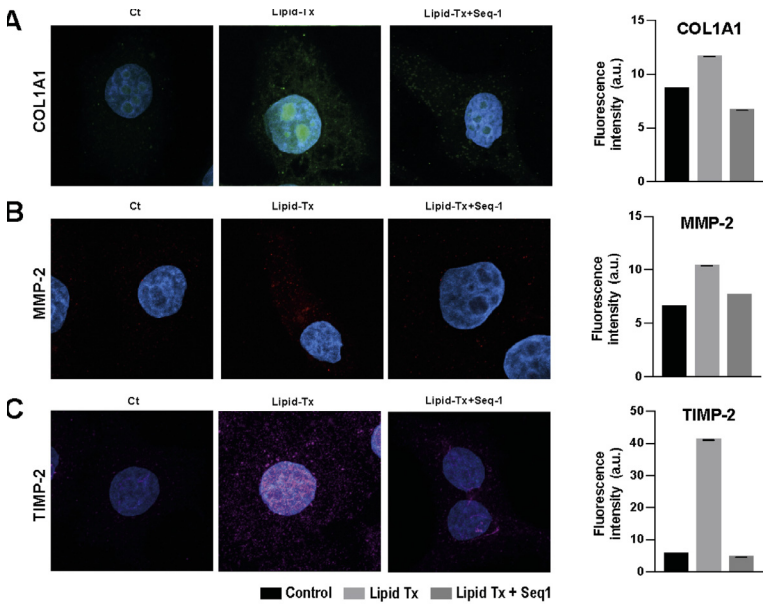

Figure 7. Immunofluorescence analysis of COL1A1, MMP-2, and TIMP-2. The experiments show a decreased expression of the three proteins in steatotic HepG2 cells plus peptide seq-1. Representative images of HepG2 cells of the three study groups A. COL1A1 (green); B. MMP-2 (red); MMP-2 (violet). Red and violet colors are pseudocolors of Alexa 488 modified after confocal acquisition using ImageJ. Values are presented as mean ± S.E.

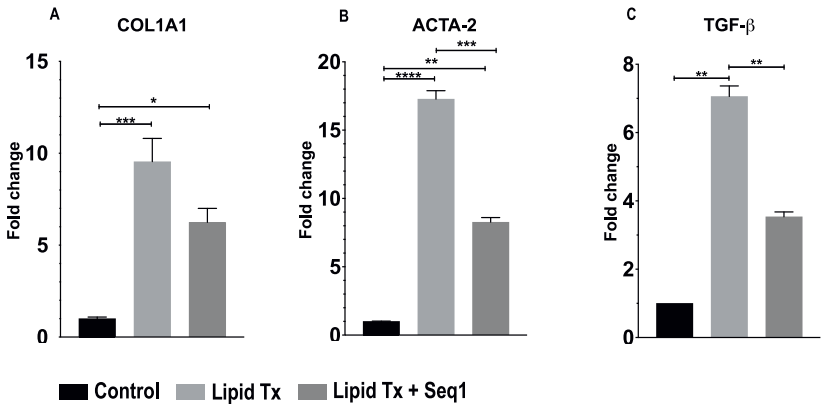

Figure 8. Steatotic hepatocyte culture media plus peptide seq-1 reduce profibrogenic expression of HCS. HSCs were incubated with the conditioned medium obtained from 2:1 palmitate/oleate-treated hepatocytes for 72 h plus the addition of 100μL of peptide seq-1. Subsequently, mRNA expression of A. COL1A1, B. ACTA2, and C. TGF-β were analyzed by qPCR analysis; $^{*}p$ <0.05; $^{**}p$ <0.01; $^{***}p$ <0.001; $^{****}p$ <0.0001.

The association between NAFLD and atherosclerosis highlights the importance of insulin resistance in both conditions. Insulin resistance affects glucose uptake by hepatocytes and impairs the ability of adipocytes to store glucose as triglycerides, leading to an increased lipolysis and the release of free fatty acids (FFAs) into the bloodstream. The FFAs are then taken up by the liver and contribute to the development of hepatic steatosis, a critical factor in the progression of atherosclerosis and cardiovascular disease (49–51).

In this context, our study established a cellular model of hepatic steatosis using a mixture of oleic and palmitic acids, the most abundant long-chain fatty acids in hepatic triglycerides in normal subjects and patients with micro- and macro-vesicular steatosis (52,53). The successful induction of lipid accumulation in HepG2 cells by this model is particularly relevant, as it can replicate the conditions associated with lipid accumulation in NASH, a disease in which lipid accumulation exceeds the body's ability to remove it. This imbalance leads to an increased hepatic fatty acid uptake, and *de novo* lipogenesis, which promotes cell damage and the progression of NAFLD by inducing oxidative stress (54,55).

To address this metabolic dysfunction, our study investigated the hepatoprotective effect of peptide Seq-1 on steatotic HepG2 cells. Employing the cellular model of hepatic steatosis, we have shown that treatment with peptide seq-1 results in a decreased level of cell glucose concentration, which is associated with a decreased triglyceride and cholesterol synthesis. As mentioned above, insulin resistance may contribute to NASH by affecting intracellular glucose levels. When cells become insulin resistant, their ability to efficiently take up glucose from the bloodstream is impaired, leading to elevated blood sugar levels and increased glucose availability within hepatocytes. High intracellular glucose levels trigger a cascade of events that promote the development of NASH. Excess glucose within the hepatocytes stimulates *de novo* lipogenesis, resulting in the synthesis of fatty acids. These fatty acids are then converted to triglycerides, which accumulate in the liver (56–58). Moreover, elevated glucose levels also activate inflammatory pathways and oxidative stress, contributing to liver inflammation and damage (59). Over time, the progression of NASH can lead to fibrosis, cirrhosis, and liver failure. In this regard, the effect of peptide seq-1 upon the regulation of the intracellular glucose and lipid levels, even in the presence of fatty acids, is particularly relevant to theoverall benefical effect of the HB-ATV-8 nasal vaccine.

As a well-known anti-inflammatory cytokine, IL-10 can activate the signal transducer and activatior of transcription 3 protein (STAT3) in Kupffer cells, effectively regulating liver inflammation (60). It has also been shown that IL-10 knockout mice have less steatosis and lower serum alanine aminotransferase (ALT) levels than control animals (61). Therefore, it is important to consider that IL-10 may have both anti-inflammatory and pro-inflammatory effects in different inflammatory contexts. Under our experimental conditions, HepG2 cells that received lipid treatment increased the synthesis of IL-10, whereas incubation in the presence of both, lipid, and peptide seq-1, returned its synthesis to basal levels, showing that IL-10 might have different roles in the cell depending on the conditions and the balance between an important number of inflammatory mediators, supporting the duality of this cytokine (62). The reduction of IL-10 expression upon stimulation with peptide seq-1 may be related to the fact that peptide treatment reduces cell damage in response to the downregulation of key markers of fibrosis. Although the significance of ICAM, VCAM, and selectin was not achieved in response to lipid treatment and further exposure to peptide seq-1, the interesting trend observed with both VCAM and selectin warrants further experimentation increasing the number of replicates.

Another crucial aspect of NASH progression is oxidative stress, known to increase in patients with NAFLD.

Oxidative stress is characterized by elevated levels of reactive oxygen species (ROS) and mitochondrial dysfunction. Excessive ROS production and lipid peroxidation products contribute to oxidative stress and mitochondrial damage (63). In the present work, we observed that the accumulation of fatty acids in steatotic HepG2 cells led to an increase in the intracellular content of ROS. Interestingly, treatment with peptide seq-1 mitigated ROS generation, potentially activating an antioxidant system to neutralize ROS and lipid peroxides.

In addition to promoting metabolic restoration through regulation of lipid, glucose, and oxidative stress, the peptide seq-1 seems to have an important role in the expression of genes and proteins directly associated with the fibrotic process in parenchymal and non-parenchymal liver cells. Since hepatocytes and HSCs play a significant role in liver dysfunction and the process of fibrogenesis, the understanding of the important signals regulating HSC activation and proliferation has become a key point in the potential control of fibrosis and liver failure.

Under non-pathological conditions, stellate cells are in a quiescent state, but when liver damage occurs, they become activated and undergo a transformation that produces extracellular matrix proteins and promotes tissue scarring (64). Stellate cell activation is triggered by various factors, including oxidative stress, cytokines, growth factors, and lipid peroxidation products (65). These factors promote the production of ROS and activate signaling pathways, including the TGF-β/Smad and NF-κB pathways that lead to this activation (66–68). In response to TGF-β, HSCs become highly proliferative during transformation, producing large amounts of extracellular matrix (ECM) proteins such as collagen, fibronectin, and laminin. In pathological conditions where hepatocytes are compromised, these ECM proteins accumulate in the liver and disrupt its normal architecture and function. This phenomenon results in the formation of fibrous tissue and the progressive loss of liver function (33–35,69). In addition to TGF-β, hepatocytes secrete other cytokines and growth factors that can influence HSC activation and proliferation. For example, the platelet-derived growth factor (PDGF), and the fibroblast growth factor (FGF) are known to stimulate HSC proliferation and collagen synthesis (70,71).

Since the relationship between hepatocytes and HSCs is complex and dynamic, a new approach is needed to fully understand this relationship and find new ways to block exacerbated HSC responses due to hepatocyte damage (72). Therefore, considering the experiments presented here and demonstrating the anti-fibrotic and anti-inflammatory effects of peptide seq-1 as the key component of the therapeutic vaccine HB-ATV-8, we can further strengthen the conclusion that HB-ATV-8 holds great promise in the prevention and potential treatment for both NASH and associated atherosclerosis.

The discovery of the anti-fibrotic properties of peptide seq-1 adds a new dimension to the therapeutic potential of HB-ATV-8 in NASH. Fibrosis, characterized by excessive deposition of extracellular matrix components in the liver, is a critical determinant of disease progression and liver dysfunction in patients with NASH. The ability of peptide seq-1 to inhibit fibrosis represents a significant breakthrough, as it suggests that HB-ATV-8 may not only address the blockade of CETP through antibody production, but may also directly target inflammation and the underlying fibrotic process by attenuating hepatic fibrosis through the downregulation of key markers in the fibrotic process, such as ACTA2, COL1A1, and TGF-B. Peptide seq-1 has the potential to improve liver function and reduce the risk of developing advanced stages of NASH, such as cirrhosis and hepatocellular carcinoma. The HB-ATV-8 vaccine may help restore the balance between pro- and anti-inflammatory factors by targeting and modulating key inflammatory pathways, effectively dampening the presence of chronic inflammation associated with NASH and atherosclerosis.

Advanced atherosclerotic plaques are characterized by the development of fibrous caps, that can become fragile and prone to rupture, leading to blood clots and subsequent cardiovascular complications. Further studies with the nasal vaccine HB-ATV-8 will need to address the possibility that, by inhibiting fibrosis within the initial lesions that lead to plaques, the treatment may contribute to stabilize the lesions and reduce the likelihood of rupture. While our experimentation provides compelling evidence for the anti-fibrotic and anti-inflammatory effects of peptide seq-1, further preclinical and clinical investigations are warranted to fully explore its preventive and therapeutic potential as part of the nasal vaccine HB-ATV-8.

In conclusion, our findings highlight the importance of peptide seq-1 in addressing the key pathological features of NASH, including lipid accumulation, insulin resistance, oxidative stress, and fibrosis. Peptide seq-1, the key component of the nasal vaccine HB-ATV-8, shows an important effect in regulating gene expression, reducing cell glucose, inhibiting triglyceride and cholesterol synthesis pathways, mitigating cell ROS generation, and preventing liver fibrosis. Supported by the present results, the HB-ATV-8 nasal vaccine consolidates itself as a new prospect in the prevention and treatment of NASH, which is directly associated with the development of cardiovascular disease.

Conflict of Interest

The authors declare the following financial interests/personal relationships which may be considered as potential competing interests: Dr. Mas-Oliva is a co-founder of and has equity in Hamol Biosolutions LLC. The other authors declare no potential conflicts of interest.

Acknowledgments

This work has been supported by PAPIIT-UNAM (IN207121 and IN209424) awarded to J M-O. S. Calixto-Tlacomulco is a Ph.D. student in the Doctoral Program in Biomedical Sciences, and I. Luna- Reyes is a Ph.D. student in the Masters and Doctorate Program in Biochemical Sciences, both at Universidad Nacional Autónoma de México. Both students have received scholarships from CONAHCyT during their graduate studies. The authors thank Paul Gaytán, Santiago Becerra, Jorge Yáñez, and Eugenio López of IBT-UNAM for the synthesis of high-quality oligonucleotides. The authors also thank Dr. Ruth Rincón Heredia for her expert advice on confocal microscopy techniques.

References

1. Perumpail BJ, Khan MA, Yoo ER, et al. Clinical epidemiology and disease burden of nonalcoholic fatty liver disease. World J Gastroenterol 2017;23:8263–8276. doi:10.3748/wjg.v23.i47.8263.
2. Bian Z, Ma X. Liver Fibrogenesis in Non-Alcoholic Steatohepatitis. Front Physiol 2012;3:248. doi:10.3389/FPHYS.2012.00248.
3. Wree A, Broderick L, Canbay A, et al. From NAFLD to NASH to cirrhosis-new insights into disease mechanisms. Nat Rev Gastroenterol Hepatol 2013;10:627–636. doi:10.1038/nrgastro.2013.149.
4. Chalasani N, Younossi Z, Lavine JE, et al. The diagnosis and management of nonalcoholic fatty liver disease: Practice guidance from the American Association for the Study of Liver Diseases. Hepatology 2018;67:328–357. doi:10.1002/HEP.29367.
5. Kotronen A, Yki-Järvinen H. Fatty liver: A novel component of the metabolic syndrome. Arterioscler Thromb Vasc Biol 2008;28:27–38. doi:10.1161/atvbaha.107.147538.
6. Targher G, Day CP, Bonora E. Risk of Cardiovascular Disease in Patients with Nonalcoholic Fatty Liver Disease. New Eng J Med 2010;363:1341–1350. doi:10.1056/nejmra0912063.
7. Avolio E, Gualtieri P, Romano L, et al. Obesity and Body Composition in Man and Woman: Associated Diseases and the New Role of Gut Microbiota. Curr Med Chem 2019;27:216–229. doi:10.2174/0929867326666190326113607.
8. Eckel RH, Alberti KGMM, Grundy SM, et al. The metabolic syndrome. The Lancet 2010;375:181–183. doi:10.1016/S0140-6736(09)61794-3.
9. Grundy SM, Cleeman JI, Daniels SR, et al. Diagnosis and management of the metabolic syndrome: an American Heart Association/National Heart, Lung, and Blood Institute Scientific Statement. Circulation 2005;112:2735–2752. doi:10.1161/circulationaha.105.169404.
10. Martin A, Lang S, Goeser T, et al. Management of Dyslipidemia in Patients with Non-Alcoholic Fatty Liver Disease. Curr Atheroscler Rep 2022;24:533–546. doi:10.1007/s11883-022-01028-4.
11. Nishihara T, Miyoshi T, Ichikawa K, et al. Association of Oxidized Low-Density Lipoprotein in Nonalcoholic Fatty Liver Disease with High-Risk Plaque on Coronary Computed Tomography Angiography: A Matched Case–Control Study. J Clin Med 2022;11:2838. doi:10.3390/jcm11102838.
12. Deprince A, Haas JT, Staels B. Dysregulated lipid metabolism links NAFLD to cardiovascular disease. Mol Metab 2020;42:101092. doi:10.1016/j.molmet.2020.101092.
13. Tilg H, Moschen AR. Evolution of inflammation in nonalcoholic fatty liver disease: the multiple parallel hits hypothesis. Hepatology 2010;52:1836–1846. doi:10.1002/hep.24001.
14. van den Hoek AM, Özsezen S, Caspers MPM, et al. Unraveling the Transcriptional Dynamics of NASH Pathogenesis Affecting Atherosclerosis. Int J Mol Sci 2022;23:8229. doi:10.3390/ijms23158229.
15. Abdallah LR, de Matos RC, e Souza YPDM, et al. Non-alcoholic Fatty Liver Disease and Its Links with Inflammation and Atherosclerosis. Curr Atheroscler Rep 2020;22:7. doi:10.1007/s11883-020-0820-8.
16. Zhang L, She ZG, Li H, et al. Non-alcoholic fatty liver disease: A metabolic burden promoting atherosclerosis. Clin Sci 2020;134:1775–1799. doi:10.1042/CS20200446.
17. Fernando DH, Forbes JM, Angus PW, et al. Development and progression of non-alcoholic fatty liver disease: The role of advanced glycation end products. Int J Mol Sci 2019;20:5037. doi:10.3390/ijms20205037.
18. Del Turco S, Basta G. An update on advanced glycation endproducts and atherosclerosis. BioFactors 2012;38:266–274. doi:10.1002/biof.1018.
19. Duan Y, Pan X, Luo J, et al. Association of Inflammatory Cytokines With Non-Alcoholic Fatty Liver Disease. Front Immunol 2022;13:880298. doi:10.3389/fimmu.2022.880298.
20. Iwakiri Y, Kim MY. Nitric oxide in liver diseases. Trends Pharm Sci 2015;1:524–536. doi:10.1016/j.tips.2015.05.001.
21. Sansbury BE, Hill BG. Regulation of obesity and insulin resistance by nitric oxide. Free Rad Biol Med 2014;73:383–399. doi:10.1016/j.freeradbiomed.2014.05.016.
22. Rodrigues Robim M, He Yong, et al. E-Selectin-Dependent Inflammation and Lipolysis in Adipose Tissue Exacerbate Steatosis-to-NASH Progression via S100A8/9. Cell Mol Gastroenterol Hepatol 2022;13:151–171. doi:10.1016/j.jcmgh.2021.08.002.
23. Kamm DR, McCommis KS. Hepatic stellate cells in physiology and pathology. J Physiol 2022;600:1825–1837. doi:10.1113/JP281061.
24. Moreira RK. Hepatic stellate cells and liver fibrosis. Arch Pathol Lab Med 2007;131:1728–1734. doi:10.5858/2007-131-1728-HSCALF.
25. Tsuchida T, Friedman SL. Mechanisms of hepatic stellate cell activation. Nature Rev Gastroenterol Hepatol 2017;14:397–411. doi:10.1038/nrgastro.2017.38.
26. Bataller R, Brenner DA. Hepatic stellate cells as a target for the treatment of liver fibrosis. Semin Liver Dis 2001;21:665–672. doi:10.1055/s-2001-17558.
27. Friedman SL. Hepatic stellate cells: protean, multifunctional, and enigmatic cells of the liver. Physiol Rev 2008;88:125–172. doi:10.1152/physrev.00013.2007.
28. Loft A, Alfaro AJ, Schmidt SF, et al. Liver-fibrosis-activated transcriptional networks govern hepatocyte reprogramming and intrahepatic communication. Cell Metab 2021;33 1685–1700.e9. doi:10.1016/j.cmet.2021.06.005.
29. Dewidar B, Meyer C, Dooley S, et al. TGF-β in Hepatic Stellate Cell Activation and Liver Fibrogenesis—Updated 2019. Cells 2019;8:1419. doi:10.3390/cells8111419.
30. Mas-Oliva J, García-González V, Delgado-Coello BA, et al. Vacuna de aplicación nasal contra el desarrollo de la enfermedad aterosclerótica y el hígado graso. MX347400B (Patent) 2017.
31. Mas-Oliva Jaime, García-González VG, Delgado-Coello BA, et al. Nasal vaccine against the development of atherosclerosis disease and fatty liver. US9539312B2 (Patent) 2017.
32. Mas-Oliva J, García-González VG, Delgado-Coello BA, et al. Nasal vaccine against the development of atherosclerosis disease and fatty liver. EP2868327A4 (Patent) 2021.
33. García-González V, Delgado-Coello B, Pérez-Torres A, et al. Reality of a Vaccine in the Prevention and Treatment of Atherosclerosis. Arch Med Res 2015;46:427–437. doi:10.1016/J.arcmed.2015.06.004.
34. Gutiérrez-Vidal R, Delgado-Coello B, Méndez-Acevedo KM, et al. Therapeutic Intranasal Vaccine HB-ATV-8 Prevents Atherogenesis

and Non-alcoholic Fatty Liver Disease in a Pig Model of Atherosclerosis. Arch Med Res 2018;49:456–470. doi:10.1016/J.ARCMED.2019.01.007.
35. Mas-Oliva J, Delgado-Coello B, Méndez-Acevedo K, et al. Preclinical evidence studying intranasal HB-ATV-8 vaccine in a porcine model of atherosclerosis shows high efficiency in the prevention of atherogenesis and fatty liver disease. Atherosclerosis 2017;263:e52. doi:10.1016/j.atherosclerosis.2017.06.177.
36. Mas-Oliva J. Molecular events involved in the efficacy of therapeutic vaccine HB-ATV-8. Atherosclerosis 2020;315:e138. doi:10.1016/j.atherosclerosis.2020.10.426.
37. Yurasov S, Wardemann H, Hammersen J, et al. Defective B cell tolerance checkpoints in systemic lupus erythematosus. J Exp Med 2005;201:703–711. doi:10.1084/jem.20042251.
38. García-González V, Gutiérrez-Quintanar N, Mendoza-Espinosa P, et al. Key structural arrangements at the C-terminus domain of CETP suggest a potential mechanism for lipid-transfer activity. J Struct Biol 2014;186:19–27. doi:10.1016/j.jsb.2014.02.002.
39. Bolaños-García VM, Soriano-García M, Mas-Oliva J. Stability of the C-terminal peptide of CETP mediated through an (i, i+4) array. Biochim Biophys Acta - Prot Struct Mol Enzymol 1998;1384:7–15. doi:10.1016/S0167-4838(97)00156-8.
40. Wang S, Wangz X, Deng L, et al. Point Mutagenesis of Carboxyl-terminal Amino Acids of Cholesteryl Ester Transfer Protein opposite faces of an amphipathic helix important for cholesteryl ester transfer or for binding neutralizing antibody. J Biol Chem 1993;268:1955–1959. doi:10.1016/S0021-9258(18)53947-8.
41. Wang S, Kussie P, Deng L, et al. Defective Binding of Neutral Lipids by a Carboxyl-terminal Deletion Mutant of Cholesteryl Ester Transfer Protein: evidence for a carboxyl-terminal cholesteryl ester binding site essential for neutral lipid transfer activity. J Biol Chem 1995;270:612–618. doi:10.1074/jbc.270.2.612.
42. Cobbold SP, Adams E, Farquhar CA, et al. Infectious tolerance via the consumption of essential amino acids and mTOR signaling. Proc Natl Acad Sci USA 2009;106:12055–12060. doi:10.1073/pnas.0903919106.
43. Ma C, Kesarwala AH, Eggert T, et al. NAFLD causes selective CD4+ T lymphocyte loss and promotes hepatocarcinogenesis. Nature 2016;531:253–257. doi:10.1038/nature16969.
44. Xia M, Wu Q, Chen P, et al. Regulatory T Cell-Related Gene Biomarkers in the Deterioration of Atherosclerosis. Front Cardiovasc Med 2021;8:661709. doi:10.3389/fcvm.2021.661709.
45. Wobser H, Dorn C, Weiss TS, et al. Lipid accumulation in hepatocytes induces fibrogenic activation of hepatic stellate cells. Cell Res 2009;19:996–1005. doi:10.1038/cr.2009.73.
46. Giraudi PJ, Barbero Becerra VJ, Marin V, et al. The importance of the interaction between hepatocyte and hepatic stellate cells in fibrogenesis induced by fatty accumulation. Exp Mol Pathol 2015;98:85–92. doi:10.1016/j.yexmp.2014.12.006.
47. Teo W, Caprariello AV, Morgan ML, et al. Nile Red fluorescence spectroscopy reports early physicochemical changes in myelin with high sensitivity. Proc Natl Acad Sci USA 2021;118:e2016897118. doi:10.1073/PNAS.2016897118.
48. Repetto G, del Peso A, Zurita JL. Neutral red uptake assay for the estimation of cell viability/cytotoxicity. Nat Protoc 2008;3:1125–1131. doi:10.1038/nprot.2008.75.
49. Fabbrini E, Magkos F, Mohammed BS, et al. Intrahepatic fat, not visceral fat, is linked with metabolic complications of obesity. Proc Natl Acad Sci USA 2009;106:15430–15435. doi:10.1073/pnas.0904944106.
50. Samuel VT, Shulman GI. The pathogenesis of insulin resistance: Integrating signaling pathways and substrate flux. J Clin Inv 2016;126:12–22. doi:10.1172/JCI77812.
51. Stefan N, Häring HU, Cusi K. Non-alcoholic fatty liver disease: causes, diagnosis, cardiometabolic consequences, and treatment strategies. Lancet Diabetes Endocrinol 2019;7:313–324. doi:10.1016/S2213-8587(18)30154-2.
52. Araya J, Rodrigo R, Videla LA, et al. Increase in long-chain polyunsaturated fatty acid n - 6/n - 3 ratio in relation to hepatic steatosis in patients with non-alcoholic fatty liver disease. Clin Sci 2004;106:635–643. doi:10.1042/CS20030326.
53. Malhi H, Gores GJ. Molecular mechanisms of lipotoxicity in nonalcoholic fatty liver disease. Semin Liver Dis 2008;28:360–369. doi:10.1055/S-0028-1091980.
54. Donnelly KL, Smith CI, Schwarzenberg SJ, et al. Sources of fatty acids stored in liver and secreted via lipoproteins in patients with nonalcoholic fatty liver disease. J Clin Invest 2005;115:1343–1351. doi:10.1172/jci23621.
55. Virtue S, Vidal-Puig A. Adipose tissue expandability, lipotoxicity and the Metabolic Syndrome–an allostatic perspective. Biochim Biophys Acta 2010;1801:338–349. doi:10.1016/j.bbalip.2009.12.006.
56. Bugianesi E, Moscatiello S, Ciaravella MF, Marchesini G. Insulin Resistance in Nonalcoholic Fatty Liver Disease. Curr Pharm Des 2010;16:1941–1951. doi:10.2174/138161210791208875.
57. Gastaldelli A, Cusi K, Pettiti M, et al. Relationship between hepatic/visceral fat and hepatic insulin resistance in nondiabetic and type 2 diabetic subjects. Gastroenterology 2007;133:496–506. doi:10.1053/j.gastro.2007.04.068.
58. Petta S, Gastaldelli A, Rebelos E, et al. Pathophysiology of Non Alcoholic Fatty Liver Disease. Int J Mol Sci 2016;17:2082. doi:10.3390/ijms17122082.
59. Wang X, Wang Z, Liu JZ, et al. Double antioxidant activities of rosiglitazone against high glucose-induced oxidative stress in hepatocyte. Tox in vitro 2011;25:839–847. doi:10.1016/j.tiv.2011.02.004.
60. Gao B. Hepatoprotective and anti-inflammatory cytokines in alcoholic liver disease. J Gastroenterol Hepatol 2012;27(Suppl.2):89–93. doi:10.1111/j.1440-1746.2011.07003.x.
61. Miller AM, Wang H, Bertola A, et al. Inflammation-associated interleukin-6/signal transducer and activator of transcription 3 activation ameliorates alcoholic and nonalcoholic fatty liver diseases in interleukin-10-deficient mice. Hepatology 2011;54:846–856. doi:10.1002/hep.24517.
62. Mocellin S, Panelli MC, Wang E, Nagorsen D, Marincola FM. The dual role of IL-10. Trends Immunol 2003;24:36–43. doi:10.1016/s1471-4906(02)00009-1.
63. McGlinchey AJ, Govaere O, Geng D, et al. Metabolic signatures across the full spectrum of non-alcoholic fatty liver disease. JHEP Reports 2022;4:100477. doi:10.1016/j.jhepr.2022.100477.
64. Hernandez-Gea V, Friedman SL. Pathogenesis of Liver Fibrosis. Ann Rev Path: Mechanisms of Disease 2011;6:425–456. doi:10.1146/annurev-pathol-011110-130246.
65. Tacke F, Weiskirchen R. Update on hepatic stellate cells: Pathogenic role in liver fibrosis and novel isolation techniques. Expert Rev Gastroenterol Hepatol 2012;6:67–80. doi:10.1586/egh.11.92.
66. Yuan Q, Tang B, Zhang C. Signaling pathways of chronic kidney diseases, implications for therapeutics. Signal Transduct Target Ther 2022;7:182. doi:10.1038/s41392-022-01036-5.
67. Pociask D, Sime P, Brody A. Asbestos-derived reactive oxygen species activate TGF-beta1. Lab Invest 2004;84:1013–1023. doi:10.1038/labinvest.3700109.
68. Jobling MF, Mott JD, Finnegan MT, et al. Isoform-specific activation of latent transforming growth factor beta (LTGF-beta) by reactive oxygen species. Radiat Res 2006;166:839–848. doi:10.1667/RR0695.1.
69. Pinzani M. Pathophysiology of Liver Fibrosis. Digestive Dis 2015;33:492–497. doi:10.1159/000374096.
70. Pinzani M. PDGF and signal transduction in hepatic stellate cells. Front Biosci 2002;7:d1720–d1726. doi:10.2741/a875.

71. Brenner DA. Molecular Pathogenesis of Liver Fibrosis. Trans Am Clin Climatol Assoc 2009;120:361–368 PMID: 19768189;PMCID: PMC2744540.

72. Zhang CY, Yuan WG, He P, et al. Liver fibrosis and hepatic stellate cells: Etiology, pathological hallmarks and therapeutic targets. World J Gastroenterol 2016;22:10512–10522. doi:10.3748/wjg.v22.i48.10512.